Composite Structures 297 (2022) 115944

Contents lists available at ScienceDirect

Composite Structures

journal homepage: www.elsevier.com/locate/compstruct

Evaluation of the interlaminar fracture toughness on composite materials using DCB test on symmetric and unsymmetric configurations

J. Cañas, J. Justo *, F. París

Grupo de Elasticidad y Resistencia de Materiales, Escuela Técnica Superior de Ingeniería, Universidad de Sevilla, Camino de los Descubrimientos s/n, 41092 Sevilla, Spain

ARTICLE INFO

Keywords:
Carbon fibre
Fracture toughness
Mechanical testing

ABSTRACT

A procedure to measure the interlaminar fracture toughness of a composite material is proposed in this work. This property is evaluated using the DCB test, the new formulation developed being applicable to small thicknesses and nonsymmetric configurations. The G_C evaluation proposed in this paper does not require to know the evolution of the crack length with the load. This fact facilitates the performance of the test and allows complex situations (crack jumps, tests at high temperature,...) to be taken under consideration. An experimental campaign has been carried out on four different configurations, three symmetric (2 + 2, 4 + 4 and 8 + 8 layers) and one nonsymmetric (4 + 8 layers). The results show that, when they are appropriately treated, the values obtained are independent of the number of layers of the adherents and even of the symmetry of the joint, validating the use of the DCB test on nonstandardized coupons.

1. Introduction

The use of adhesive joints in composites has been pursued, instead of bolted joints, since the beginning of using these materials, as the first saves weight and manufacturing operations. Even better than adhesive joints is the integration of the parts through cocuring operations, in which the different parts of an structure are cured at the same time. In this case, the weight savings are higher and the bonding is completely chemical. A crucial factor needed in the design of this type of integrated structures is the interlaminar fracture toughness energy in mode I (G_{1C}) of the material, that is, the energy needed to propagate a crack throughout the joint in mode I.

Traditionally, the interlaminar fracture toughness has been evaluated by a peeling test, consisting on subjecting a specimen that presents a crack to a force at its ends that causes the propagation of the crack.

The evaluation of the interlaminar fracture toughness of a composite laminate is carried out by measuring the energy released per unit area when a crack propagates throughout two layers.

$$G_C = \frac{1}{B}\left(\frac{\Delta W}{\Delta a} - \frac{\Delta U}{\Delta a}\right) \tag{1}$$

where B is the width of the coupon, a is the length of the crack, W is the work of the external loads and U is the internal strain energy.

The most common test to measure G_C is the DCB test (double cantilever beam) [1,2,3]. This test, according to the standards, can only be carried out on symmetric configurations and when the thicknesses of the adherents are between 1.5 mm and 2.5 mm. For the case of smaller thicknesses, the theory of large displacements must be taken into account. The ASTM standard [1] proposes several corrections to take into consideration not only the effect of large displacements, but also the effect introduced by the loading blocks.

The objective of this work is to propose a calculation procedure to obtain G_{1C} on DCB coupons valid for the most general situation, contemplating nonsymmetric configurations, effect of the loading blocks and small thickness of the adherents. The procedure proposed does not require to measure the crack length, which supposes a great advantage over the traditional procedures since there is great uncertainty in this measurement, and even its determination can be very complicated if not impossible (e.g. tests within a climatic chamber at temperature other than ambient).

To verify the validity of the procedure, an experimental campaign has been carried out, calculating the fracture toughness values by traditional and proposed procedures. For nonsymmetric coupons, a fracture toughness correction, based on a phenomenological law of Hutchison and Suo [4] and on a measurement of the mixicity angle based on the work of Cañas et al. [5], is used to obtain G_{1C}.

* Corresponding author.
E-mail address: jjusto@us.es (J. Justo).

https://doi.org/10.1016/j.compstruct.2022.115944
Received 9 February 2022; Received in revised form 18 May 2022; Accepted 18 June 2022
Available online 27 June 2022

2. DCB test

2.1. Description of the test

The test (Fig. 1a) consists on subjecting a "precracked" specimen to a peeling force until the crack propagation is achieved. To this end, a universal testing machine and a tool to grip the specimen are used. During propagation, the force and displacement of the crosshead of the testing machine and the crack length are recorded for different load levels. The standardized test (ASTM D5228, ISO 15024, AITM1-0053) [1, 2 and 3] is carried out for symmetrical configurations (identical laminates on both sides of the crack) and in this case the G_C value coincides with G_{1C} (interlaminar fracture toughness in Mode I).

A typical P-δ curve is shown in Fig. 1b. In this study, we will only deal with the evaluation of G_C in the propagation phase (after the initiation phase of the crack).

2.2. G_{1C} calculation according to standards

The value of G_{1C}, neglecting the deformation due to axial and shear forces, is given by [6,7,8]:

$$G_{1C} = \frac{M^2}{BEI} \tag{2}$$

M being the bending moment existing in each laminate at the crack tip when the crack growth is produced, and EI being the bending stiffness of each laminate. Using the small displacements hypothesis (valid for $\delta/a < 0.4$ according to ASTM, δ being the separation of the adherents at the gripping zone) and neglecting the deformation associated with the shear force, the elastic solution of the cantilever beam is [9,10]:

$$M \cong Pa \quad ; \quad \delta = \frac{2}{3}\frac{Pa^3}{EI} \tag{3}$$

Substituting in Eq. (2) it leads to:

$$G_{1C}(P,\delta,a) = \frac{3}{2}\frac{\delta P}{Ba} \tag{4}$$

Again, the evaluation of G_{1C} requires not only knowing P and δ but also the value of a for the δ considered. In this case, the advantage of Eq. (4) is that it is not necessary to measure the specimen dimensions or to know the longitudinal elastic modulus or flexural modulus of the material.

Due to reasons that will be discussed later, the measurement of a during the test is not exempt from problems.

Concerning previous equation, ASTM or ISO standards [1,2] establish several corrections (F, N and Δa) [1,9], obtaining, in this way, a corrected value of the interlaminar fracture toughness G^*_{1C}:

$$G^*_{1C}(P,\delta,a) = \frac{3}{2}\frac{P}{B}\frac{\delta}{a+\Delta a}\frac{F}{N} = G_{1C}(P,\delta,a,\Delta a)\frac{F}{N} \tag{5}$$

Regarding this formulation:

- It considers that the crack border is not clamped. The value of a is corrected, by an adjustment of experimental results, to be $a + \Delta a$, where Δa is obtained from the intersection with the X-axis of the straight line of minimun squares associated with the graph crack length (a) versus the cubic root of δ/PN (Fig. 2). N is a dimensonless factor that will be defined later.
- It considers large displacements. The value of G_{1C} is multiplied by a dimensionless factor F that depends on the quotient δ/a and the dimensions of the clamping system (see Fig. 2).

$$F = 1 - \frac{3}{10}\left(\frac{\delta}{a}\right)^2 - \frac{3}{2}\left(\frac{\delta\,(t+0.5h)}{a^2}\right) \tag{6}$$

- It considers the effect of the clamping system. The value of G_{1C} is corrected dividing it by a dimensionless factor N that depends on the dimensions of the clamping system, a and δ.

$$N = 1 - \left(\frac{c}{a}\right)^3 - \frac{9}{8}\left[1 - \left(\frac{c}{a}\right)^2\right]\left(\frac{\delta\,(t+0.5h)}{a^2}\right) - \frac{9}{25}\left(\frac{\delta}{a}\right)^2 \tag{7}$$

In any case, the expression requires to measure the crack length. Combining adequately Eqs. (2) and (3), it would be possible to obtain other expressions not involving either crack length (a) or the opening displacement (δ) [11,12,13,14], and taking into account the correction on a, several expressions of G_{1C} can be obtained (ecs. (8)–(11)). It can be seen that Eq. (10) does not depend on a, which supposes a great advantage, a priori. The main drawback of using Eq. (10) instead of Eq. (8), is that (10) requires to know the dimensions of the specimen (I =

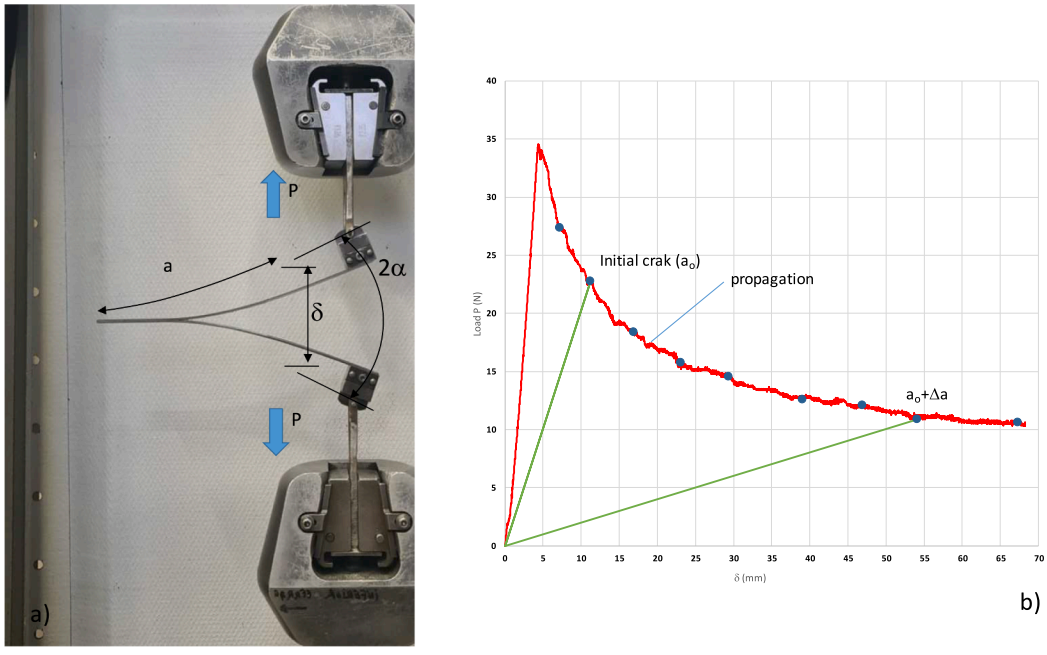

Fig. 1. (a) DCB test, (b) Typical P-δ curve from DCB test.

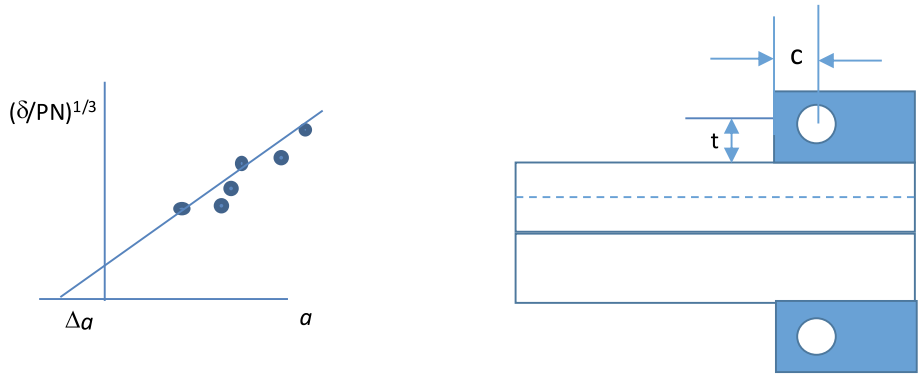

Fig. 2. Graph used to correct the crack length a and dimensions of the gripping system.

$Bh^3/12$, h being the thickness of the adherent) and the flexural elastic modulus (E).

$$G_{1C}(P,\delta,a,\Delta a) = \frac{3}{2}\frac{P}{B}\frac{\delta}{a+\Delta a} \tag{8}$$

$$G_{1C}(P,a,\Delta a,EI) = \frac{P^2(a+\Delta a)^2}{BEI} \tag{9}$$

$$G_{1C}(P,\delta,EI) = \frac{P^2}{BEI}\sqrt[3]{\left(\frac{3EI\,\delta}{2P}\right)^2} \tag{10}$$

$$G_{1C}(\delta,a,\Delta a,EI) = \frac{9}{4}\frac{EI}{B}\frac{\delta^2}{(a+\Delta a)^4} \tag{11}$$

Eqs. (9) and (11) do not present any advantage on Eq. (8) as P and δ are obtained easily from the test and with a high accuracy.

It is obvious that, if the value of a is properly measured and the small displacements hypothesis is met, all previous expressions should lead to the same value of G_{1C}. If the displacements are not small enough and the size of the clamping system is relevant, correction factors should be applied, leading to the following expressions of Eqs. (8) and (10):

$$G^*_{1C}(P,\delta,a) = G_{1C}(P,\delta,a,\Delta a)\frac{F}{N} \tag{12}$$

$$G^*_{1C}(P,\delta,EI) = G_{1C}(P,\delta,EI)\frac{F}{N^{2/3}} \tag{13}$$

It has to be noticed that, even with this procedure, the dependency on a continues, as F and N depend on it. An alternative to this drawback is to generate a procedure for large displacements (with or without the correction due to the clamping system) to determine G_{1C} just from the values of P, δ and EI.

Other standards evaluate G_{1C} (for example [3]) from the area enclosed under the P-δ curve between two values of a:

$$G_{1C} = \frac{A}{B\Delta a} \tag{14}$$

where A is the area formed by the curve P-δ and the lines that join the points with crack lengths a_o (50 mm) and $a_o + \Delta a$ with the coordinate's origin (energy required to propagate the crack), B is the width of the specimen and Δa is the increase in the crack length between the two points considered (the standard takes $\Delta a = 60$ mm).

The main drawbacks of these standardized procedures are two:

(a) They need the crack length to be measured and it can be a difficult task, especially when the curve is not smooth and there exists jumps (stick–slip) or when the test is carried out inside a climatic chamber.

(b) When the small displacements hypothesis is not met (small thickness of the adherents <1 mm), the unload (straight line between a certain point in the curve and the origin) is not linear, not being easy to determine the area A in this case.

2.3. Evaluation of interlaminar fracture toughness on DCB test for symmetrical and nonsymmetrical configurations.

The general study of the behavior of a 'beam' that presents a crack and is subjected to a load that produces the bending of its two semicoupons is presented in this section. Fig. 3 shows the general scheme of the case to be analyzed. The specimen has width B, total thickness ($h_1 + h_2$), and has two rigid blocks at its ends that are adhered to the two semicoupons. The total length of the crack is $a = a^* + c$, the material at both sides of the crack being, in accordance with Fig. 3, the same.

We will also admit that the edge of the crack is clamped, that is, the sections of the two semicoupons at the crack tip do not rotate or rotate the same for nonsymmetrical configurations. This last hypothesis could be relaxed (Kanninen [15,16]) by modeling the interface between the two semicoupons in the noncracked zone by means of a distribution of springs in the interface. A discussion concerning the stiffness values of the springs to be used is presented by Cañas et al. [5].

It should be noted that if the evaluation of G_C is performed only from P and δ, the value of a can be determined. This value of a would be a theoretical value that would correspond to the value of a for which the section does not rotate and that, in general, will be slightly higher than the real value of a.

We admit that the deformations associated with axial and shear forces are negligible compared to those from the bending moment, and that for curvature calculation purposes, only the bending moment is relevant. To obtain it, the flexural modulus, E_f, and the inertia of the section, $I = Bh_i^3/12$, $i = 1,2$, are used. In line with the considerations made above, we will assume that the effect of the shear and axial forces on the elastic energy is negligible, depending it only on the bending moment.

It is also accepted that the thicknesses of the two semicoupons (h_1 and h_2) are maintained during the propagation process, that is, the crack does not migrate.

The test is carried out using a constant displacement ratio, and the value of G_C is given by:

$$G_C = -\frac{1}{B}\frac{dU}{da} \tag{15}$$

U being the energy stored in the coupon for a certain load. As loading blocks are considered infinitely rigid, the contribution to deformation due to bending of the zone joined to the loading blocks is ignored.

For the symmetric configurations, the value of G_C (coincident with G_{1C}) as a function of the bending moment at the crack tip is given by equation (2). For the nonsymmetric configurations the expression is:

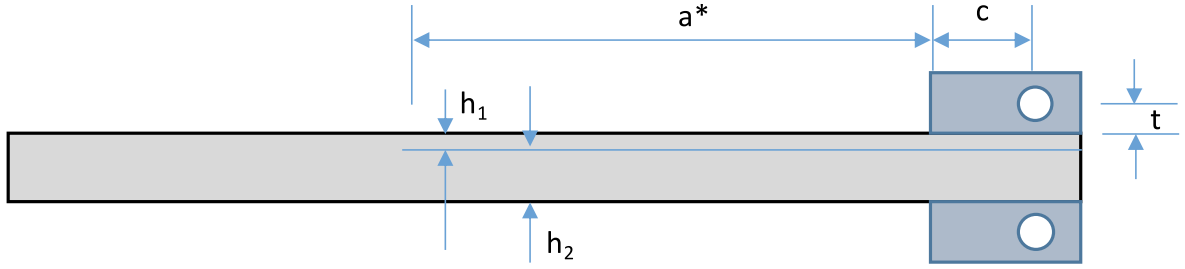

Fig. 3. Scheme of the DCB coupon with its main dimensions.

$$G_C = \frac{1}{2B}\left(\frac{M_1^2}{E_f I_1} + \frac{M_2^2}{E_f I_2}\right) \tag{16}$$

M_1 and M_2 being the bending moments at the crack tip for the upper and lower laminates, respectively.

On next subsections, the calculation of the bending moment M is described, both for symmetric and nonsymmetric configurations, considering large displacements theory and the effect of the loading blocks.

2.3.1. General formulation for the symmetric configurations (GFS)

For symmetric configurations, the formulation, using the theory of large displacements, that allows G_{1C} to be obtained was developed by Williams [8]. He took into account the effect of the loading blocks but considered that the curvature does not change with the load. This fact is taken into account in Pavelko et al. [17], who generalized Williams' work.

The differential equation for the bending moment of the semicoupon (Fig. 4) is given by:

$$EI\frac{d\theta}{ds} = M(s) = M_o - Px \tag{17}$$

With reference to Fig. 4, s_o is the generic position of the inflection point of the deformed shape (at that point $M = 0$) and α_o is the angle that the mean line of the thickness forms with the horizontal line. θ is the angle rotated by the section that is distant s from the clamping and $M(s)$ is the bending moment in that section. The value of $M(s)$, a, and δ for a given load is expressed as [17]:

$$M_o = \frac{\sqrt{2}P}{K}\sqrt{\sin\alpha_o} \tag{18}$$

$$x = \frac{\frac{M_o}{EI} - \sqrt{\left(\frac{M_o}{EI}\right)^2 - 2K^2\sin\theta}}{K^2} \tag{19}$$

$$M(s) = M_o - Px \tag{20}$$

$$a = c + \frac{1}{\sqrt{2}K}\begin{vmatrix} I_a(0,\alpha) & for & \alpha \leqslant \alpha^* \\ I_a(0,\alpha_o) + I_a(\alpha,\alpha_o) & for & \alpha \geqslant \alpha^* \end{vmatrix} \tag{21}$$

$I_a(\alpha_1,\alpha_2)$ and K being:

$$I_a(\alpha_1,\alpha_2) = \int_{\alpha_1}^{\alpha_2} \frac{d\theta}{\sqrt{\sin\alpha_o - \sin\theta}} \quad ; \quad K = \sqrt{\frac{P}{E_f I}} \tag{22}$$

The vertical displacement (δ) can be obtained as:

$$\delta = 2\left(t + \frac{h}{2}\right)(\cos\alpha - 1) + 2c\sin\alpha + 2\delta_1$$

$$\delta_1 = \frac{1}{\sqrt{2}K}\begin{vmatrix} \sin\alpha_o I_a(0,\alpha) - I_\delta(0,\alpha) & for & \alpha \leqslant \alpha^* \\ \sin\alpha_o I_a(0,\alpha_0) - I_\delta(0,\alpha_o) + \sin\alpha_o I_a(\alpha,\alpha_o) - I_\delta(\alpha,\alpha_o) & for & \alpha \geqslant \alpha^* \end{vmatrix} \tag{23}$$

$I_\delta(\alpha_1,\alpha_2)$ being:

$$I_\delta(\alpha_1,\alpha_2) = \int_{\alpha_1}^{\alpha_2} \sqrt{\sin\alpha_o - \sin\theta}\, d\theta \tag{24}$$

If $\alpha^* > \alpha \Rightarrow s_o$ (inflection point) is greater than a^*, α^* being $arctg(c/t)$.

Integrals (22) and (24) are improper integrals and their numerical resolution is more precise if they are transformed into elliptic integrals of the first and second order by making an appropriate change of variables:

$$\sin\left[\frac{1}{2}\left(\theta + \frac{\pi}{2}\right)\right] = p\sin\phi \quad ; \quad p = \sin\left[\frac{1}{2}\left(\alpha_o + \frac{\pi}{2}\right)\right] \tag{25}$$

For a given value of P and δ, Eq. (23) allow the value of α_o (or α) to be obtained, (using, for example, a simple script programmed in Wolfram Mathematica ©). Once α_o (or α) is known, Eq. (21) allow a to be obtained.

The value of G_{1C}, according to (2) and (15) is given by:

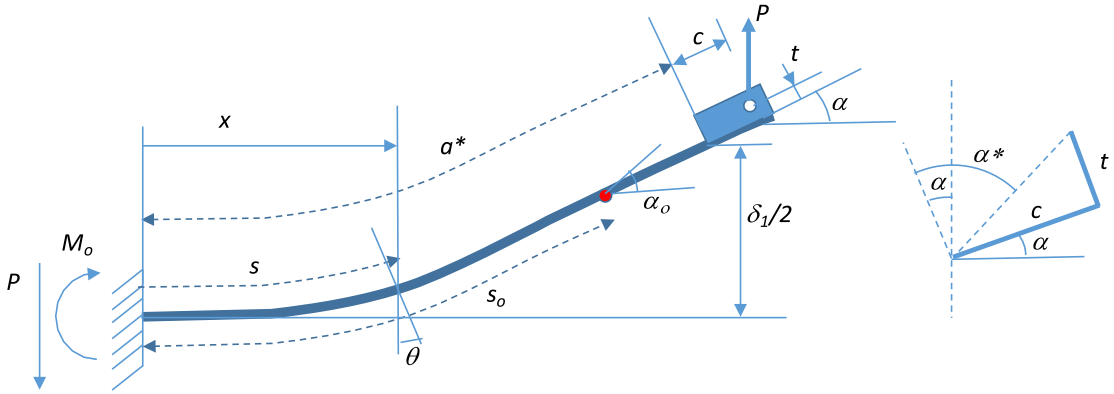

Fig. 4. Deformed shape of a DCB semicoupon.

$$G_{1C} = \frac{M_o^2}{BE_f I} = \frac{2P}{B}\sin\alpha_o \tag{26}$$

An approach based on J-integral can also be followed, as it can intrisically take large displacements under consideration. Xu and Ding [18,19] obtained an expression similar to equation (26), and identical just in the case of having no inflexion points in the deformed shape ($\alpha_o = \alpha$). They compare their results obtained with the J integral approach with those obtained from equation (26), for a case with no inflexion points, obtaining similar results.

2.3.2. New general formulation for nonsymmetric configurations (GFNS)

The standard DCB test does not contemplate this situation. It is important to notice that the absence of symmetry can cause a mixity of fracture modes, consequently, the fracture toughness value that would be obtained is G_C and not G_{1C}. Another field of application of this kind of configurations is when, even beginning with a symmetric configuration, the crack migrates during its propagation, breaking the symmetry.

Fig. 5 shows the effect of the configuration of the specimen tested. Fig. 5a shows the case of a symmetric configuration and Fig. 5b the case of a nonsymmetric configuration.

The formulation of this problem was carried out by Sundararaman [20] but without taking into account the effect of the blocks. We here present the governing equations of the problem taking into account the loading blocks, using the equations already developed in the previous section. The bending stiffnesses of the two semicoupons will be given by EI_1 and EI_2, respectively.

Thus, in relation to the scheme of Fig. 6, and the equations developed for the symmetric case, the equations that allow the problem to be solved are:

$$\delta = \frac{h_1+h_2}{2}(\cos\beta - 1) + (t + \frac{h_1}{2})(\cos\alpha_1 - 1) + (t + \frac{h_2}{2})(\cos\alpha_2 - 1) + c(\sin\alpha_2 + \sin\alpha_1) + \delta_1 + \delta_2 \tag{27}$$

$$\bar{x}_2 - \bar{x}_1 = \frac{h_1+h_2}{2}\sin\beta \tag{28}$$

$$a_1 = a_2 \tag{29}$$

where:

$$\delta_1 = \frac{1}{\sqrt{2}K_1}\begin{cases} \sin\alpha_{01} I_{a1}(-\beta,\alpha_1) - I_{\delta 1}(-\beta,\alpha_1) & for \quad \alpha_1 \leqslant \alpha_1^* \\ \sin\alpha_o I_{a1}(-\beta,\alpha_{01}) - I_{\delta 1}(-\beta,\alpha_{01}) + \sin\alpha_{01} I_{a1}(\alpha_1,\alpha_{01}) - I_{\delta 1}(\alpha,\alpha_{01}) & for \quad \alpha_1 \geqslant \alpha_1^* \end{cases}$$
$$\delta_2 = \frac{1}{\sqrt{2}K_2}\begin{cases} \sin\alpha_{02} I_{a2}(\beta,\alpha_2) - I_{\delta 2}(\beta,\alpha_2) & for \quad \alpha_2 \leqslant \alpha_2^* \\ \sin\alpha_o I_{a2}(\beta,\alpha_{02}) - I_{\delta 2}(\beta,\alpha_{02}) + \sin\alpha_{02} I_{a2}(\alpha_2,\alpha_{02}) - I_{\delta 2}(\alpha,\alpha_{01}) & for \quad \alpha_2 \geqslant \alpha_2^* \end{cases} \tag{30}$$

$$a_1 = c + \frac{1}{\sqrt{2}K_1}\begin{cases} I_{a1}(-\beta,\alpha_1) & for \quad \alpha_1 \leqslant \alpha_1^* \\ I_{a1}(-\beta,\alpha_{01}) + I_{a1}(\alpha_1,\alpha_{01}) & for \quad \alpha_1 \geqslant \alpha_1^* \end{cases}$$
$$a_2 = c + \frac{1}{\sqrt{2}K_2}\begin{cases} I_{a2}(\beta,\alpha_2) & for \quad \alpha_2 \leqslant \alpha_2^* \\ I_{a2}(\beta,\alpha_{02}) + I_{a2}(\alpha_2,\alpha_{02}) & for \quad \alpha_2 \geqslant \alpha_2^* \end{cases} \tag{31}$$

$$\bar{x}_1 = \frac{\sqrt{2}}{K_1}\sqrt{\sin\alpha_{01} + \sin\beta}$$
$$\bar{x}_2 = \frac{\sqrt{2}}{K_2}\sqrt{\sin\alpha_{02} - \sin\beta} \tag{32}$$

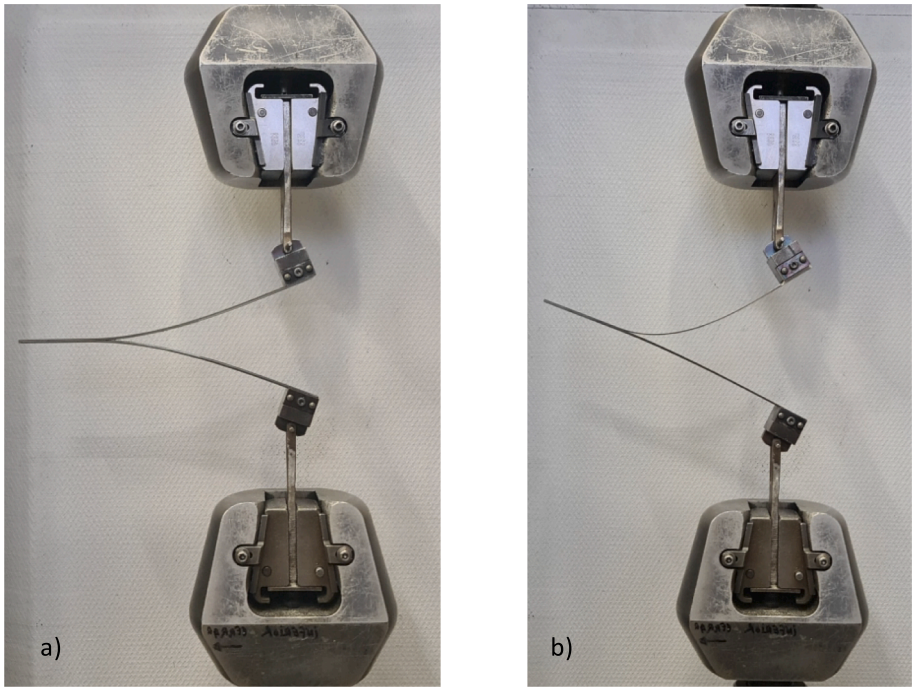

Fig. 5. Effect of the loss of symmetry during the DCB test. (a) Symmetric case ($h_1 = h_2$), (b) Nonsymmetric case ($h_2 = 2\ h_1$).

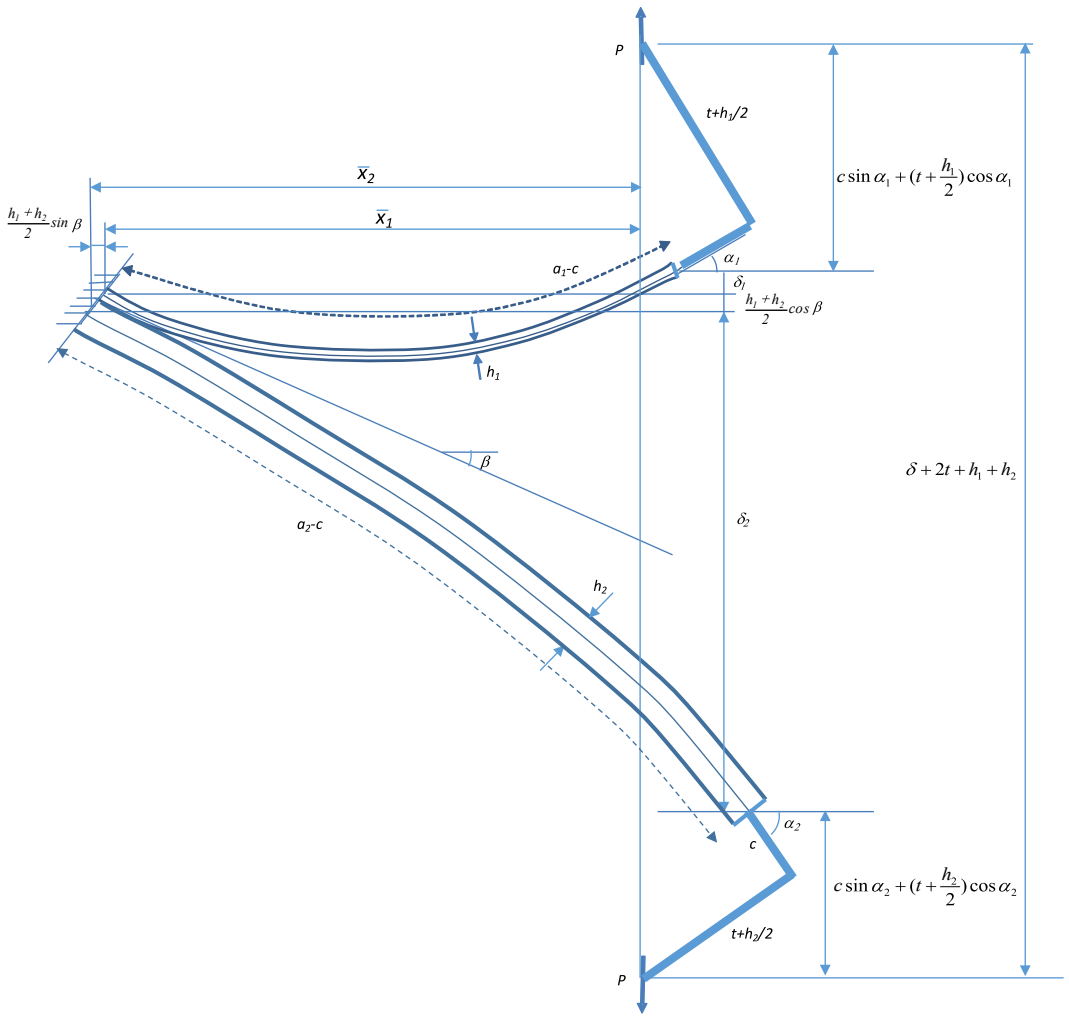

Fig. 6. Deformed shape of the coupon for a general nonsymmetric configuration.

where:

$$K_1=\sqrt{\frac{P}{E_fI_1}}\quad;\quad K_2=\sqrt{\frac{P}{E_fI_2}} \tag{33}$$

$$I_{\delta1}(\alpha_1,\alpha_2)=\int_{\alpha_1}^{\alpha_2}\sqrt{\sin\alpha_{01}-\sin\theta}d\theta\quad;\quad I_{\delta2}(\alpha_1,\alpha_2)=\int_{\alpha_1}^{\alpha_2}\sqrt{\sin\alpha_{02}-\sin\theta}d\theta \tag{34}$$

$$I_{a1}(\alpha_1,\alpha_2)=\int_{\alpha_1}^{\alpha_2}\frac{d\theta}{\sqrt{\sin\alpha_{01}-\sin\theta}}\quad;\quad I_{a2}(\alpha_1,\alpha_2)=\int_{\alpha_1}^{\alpha_2}\frac{d\theta}{\sqrt{\sin\alpha_{02}-\sin\theta}} \tag{35}$$

The solution of (27), (28) and (29) allows α_1, α_2 and β to be obtained for a given P and δ. Once these values are known, G_C can be calculated using Eq. (16):

$$G_C=\frac{1}{2B}\left(\frac{M_1^2}{E_fI_1}+\frac{M_2^2}{E_fI_2}\right)=\frac{1}{2B}\left(\frac{(P\bar{x}_1)^2}{E_fI_1}+\frac{(P\bar{x}_2)^2}{E_fI_2}\right)=\frac{P}{B}(\sin\alpha_{01}+\sin\alpha_{02}) \tag{36}$$

From Eq. (31) the value of a can be calculated (a_c). This value represents the crack length measured from the loading application point to the section that does not rotate.

It has to be noticed the, from this formulation, several particular situations can be derived. Thus, for the symmetric case, we just need to solve Eqs. (27), (28) and (29), K_1 being equal to K_2 and for the case that one of the adherents is infinitely rigid it is just needed to choose a very high value of the elastic modulus for this adherent (for example 10^6 times the modulus of the flexible adherent). Nevertheless, due to the strong nonlinearity of the equations, it is preferable to use the specific equations, which are summarized next:

Symmetric case: $h_1=h_2=h$, $K_1=K_2=K$, $\alpha_1=\alpha_2=\alpha$; $\alpha_{01}=\alpha_{02}=\alpha_0$; $\beta=0$

α_1 is the unique unknown and can be obtained from Eq. (27), which for this case is expressed as:

$$\delta=2(t+\frac{h}{2})(\cos\alpha-1)+2c\sin\alpha+2\delta_1$$
$$\delta_1=\frac{1}{\sqrt{2}K}\begin{cases}\sin\alpha_0 I_{a1}(0,\alpha)-I_{\delta1}(0,\alpha)\ \ for\ \ \alpha\leqslant\alpha^*\\ \sin\alpha_o I_{a1}(0,\alpha_0)-I_{\delta1}(0,\alpha_0)+\sin\alpha_0 I_{a1}(\alpha,\alpha_0)-I_{\delta1}(\alpha,\alpha_0)\ \ for\ \ \alpha\geqslant\alpha^*\end{cases} \tag{37}$$

Note that this equation is identical to Eq. (23).

Nonsymmetric case with the lowest adherent infinitely rigid: $K_2=0$, $\alpha_2=\beta$

Now we have two unknowns, α_1 and β, which are obtained from Eqs. (27) and (28), which for this case are expressed as:

$$\delta=\frac{h_1+h_2}{2}(\cos\beta-1)+(t+\frac{h_1}{2})(\cos\alpha_1-1)+(t+\frac{h_2}{2})(\cos\beta-1)+c(\sin\beta+\sin\alpha_1)+\delta_1+(a_1-c)\sin\beta \tag{38}$$

$$a_1\cos\beta - \left(t+\frac{h_2}{2}\right)\sin\beta - \bar{x}_1 = \frac{h_1+h_2}{2}\sin\beta \tag{39}$$

$$\delta_1 = \frac{1}{\sqrt{2}K_1}\begin{vmatrix} \sin\alpha_{01}I_{a1}(-\beta,\alpha_1) - I_{\delta 1}(-\beta,\alpha_1) & for \quad \alpha_1 \leqslant \alpha_1{}^* \\ \sin\alpha_o I_{a1}(-\beta,\alpha_{01}) - I_{\delta 1}(-\beta,\alpha_{01}) + \sin\alpha_{01}I_{a1}(\alpha_1,\alpha_{01}) - I_{\delta 1}(\alpha,\alpha_{01}) & for \quad \alpha_1 \geqslant \alpha_1{}^* \end{vmatrix} \tag{40}$$

$$a_1 = c + \frac{1}{\sqrt{2}K_1}\begin{vmatrix} I_{a1}(-\beta,\alpha_1) & for \quad \alpha_1 \leqslant \alpha_1{}^* \\ I_{a1}(-\beta,\alpha_{01}) + I_{a1}(\alpha_1,\alpha_{01}) & for \quad \alpha_1 \geqslant \alpha_1{}^* \end{vmatrix} \tag{41}$$

$$\bar{x}_1 = \frac{\sqrt{2}}{K_1}\sqrt{\sin\alpha_{01}+\sin\beta} \tag{42}$$

$$G_C = \frac{P}{B}(\sin\alpha_{01}+\sin\beta) \tag{43}$$

If the loading blocks do not exist or their dimensions are very small (for example with a gripping system like piano hinges) it is just needed to do $c = t = 0$ to adapt the former expressions.

3. Experimental results

The tests have been carried out on unidirectional carbon-epoxy laminates. The panels, from which the coupons have been extracted, have been manufactured by co-curing in an autoclave. The initial crack has been artificially generated, during the manufacturing process, by using a demolding layer. Once the panels are cured, an ultrasonic inspection of them was carried out by means of manual Pulse-Echo to rule out possible previous delaminations and to check the tip of the generated crack.

With the experimental campaign we study the following aspects:

- o Evaluation of G_{1C} following ASTM standard using P, δ and a
- o Evaluation of G_{1C} using P, δ and a and the correction factors (F and N) given by ASTM
- o Evaluation of G_{1C} using the general formulation (GFS) from symmetric configurations based on P and δ
- o Evaluation of G_{1C} from a nonsymmetric configuration using GFNS
- o Comparison of the estimated and measured crack lengths
- o Validation of the GFNS for the nonsymmetric case
- o Study of the influence of the loading blocks on the estimation of G_{1C}
- o Study of the influence of E_f on the estimation of G_{1C}

The material used in this work is a carbon-epoxy prepreg of standard modulus, curing temperature 180 °C and designation HEXPLY M21/34%/UD194/IMA-12k.

To have precise data of the flexural modulus E_f, a bending test campaign on specimens with different thicknesses (from 12 plies (2.28 mm) till 2 plies (0.38 mm), based on ISO 14125 standard [21], has been performed. The value obtained has been $E_f = 140$ GPa (±1 GPa). The tensile properties in the direction of the fibres have been obtained from tensile tests on 3 coupons, following EN 2561 standard [22] and in the direction perpendicular to the fibres using EN 2597 standard [23]. The values obtained are $E_{11} = 165$ GPa; $E_{22} = 9.3$ GPa and $\nu_{12} = 0.3$.

The thickness of each lamina has been taken $t_{lam} = 0.190$ mm, obtained from the thicknesses of the coupons used for characterization of the material.

Four configurations have been studied for the DCB test:

Configuration 1: 8 + 8 layers. Total thickness of each laminate 1.53 mm.
Configuration 2: 4 + 4 layers. Total thickness of each laminate 0.76 mm
Configuration 3: 2 + 2 layers. Total thickness of each laminate 0.38 mm.
Configuration 4: 4 + 8 layers. Total thickness of each laminate 0.76 and 1.53 mm, respectively.

Once the panels were cured, the specimens were cut by means of a diamond disc saw. All specimens are 25 mm wide.

The gripping of the specimens to the testing machine has been carried out with loading blocks such as those shown in Fig. 7, which grab laterally and therefore do not require the use of a fixing adhesive. For the 2 and 4-layers specimens, a 2.6 mm thick plate has been bonded to the end of the specimen to facilitate the holding of the blocks. The dimensions of the loading blocks are $t = 27.2$ and $c = 12.5$ mm, Fig. 7.

The tests were carried out on an INSTRON 4482 universal machine. The test parameters are those contemplated by the ASTM standard (crosshead displacement speed between 1 and 5 mm/min). The load (P) and crosshead displacement (δ) were continuously recorded. Before carrying out the test, marks were made on the thickness in order to check the evolution of the crack and thus be able to record the crack length (a_m). To better visualize the progress of the crack, a macroscopic video camera has been used.

Fig. 5 shows the test of a symmetric coupon of medium stiffness (4 + 4 layers) and a nonsymmetric coupon (4 + 8 layers).

Fig. 8 summarizes the P-δ curves for all the configurations and coupons. A small dispersion can be observed between coupons of the same number of layers. The evolution is, in all cases, both in the initiation as in

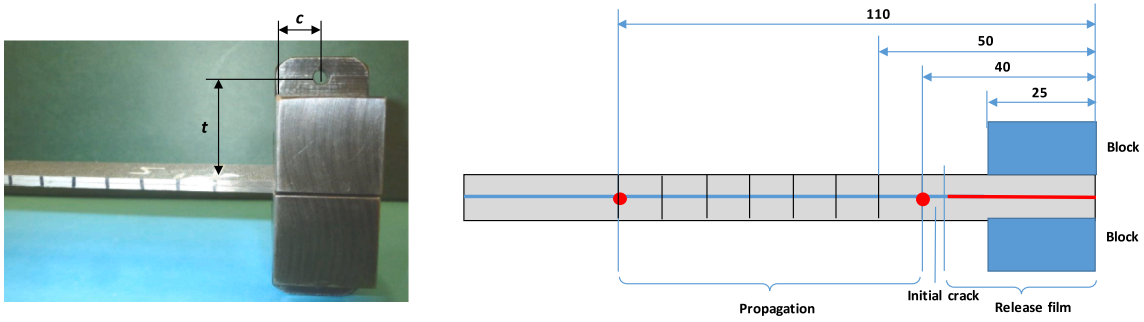

Fig. 7. Loading blocks and main lengths on the DCB test.

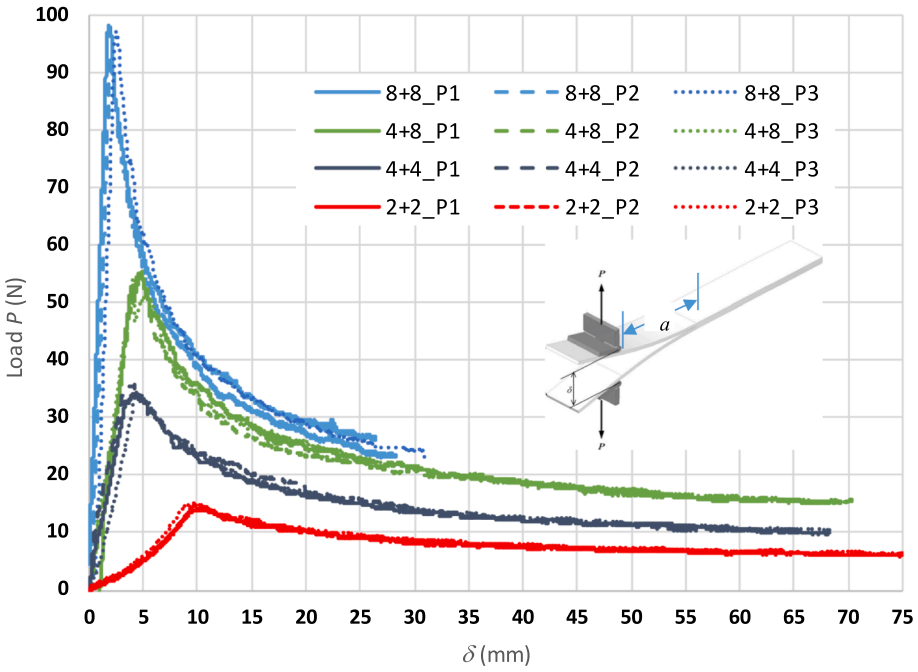

Fig. 8. *P-δ* curves of all configurations.

Table 1
Experimental *P (N)*, *δ* (mm) and *a* (mm) values of the symmetric configurations.

	8 Layers						4 Layers						2 Layers					
	8_1		8_2		8_3		4_1		4_2		4_3		2_1		2_2		2_3	
a_m	*P*	*δ*	*P*	*δ*	*P*	*δ*	*P*	*δ*	*P*	*δ*	*P*	*δ*	*P*	*δ*	*P*	*δ*	*P*	*δ*
57.5	48.5	7.0	45.4	7.6	49.5	7.1	17.7	17.8	19.4	16.6	18.4	16.9	7.7	36.0	7.9	37.1	8.1	36.5
67.5	43.1	9.3	39.4	9.8	41.5	9.6	15.5	23.2	16.1	23.1	15.8	23.1	6.9	47.2	7.1	47.2	7.4	47.3
77.5	37.7	12.0	33.8	12.3	36.5	12.2	13.8	28.9	14.4	28.7	14.6	29.4	6.5	60.4	6.5	62.7	6.9	61.6
87.5	33.7	14.8	30.8	15.7	33.3	14.8	12.7	37.3	12.8	35.4	12.6	39.1	6.1	77.1	5.9	79.8	6.4	78.5
97.5	30.4	18.1	27.7	19.8	29.7	18.4	11.5	45.8	11.5	45.2	12.1	46.9	5.7	92.5	5.7	92.7	6.0	92.3
107.5	28.1	21.9	25.3	23.6	27.6	22.0	10.8	57.1	10.5	53.7	10.9	54.1	5.8	110.3	5.4	111.8	5.6	110.9

Table 2
Calculation of G_{1C} (J/m^2) using the traditional methods described in the standards without and with the corrections.

	$G_{1C}(P,\delta,a,\Delta a) = \frac{3}{2}\frac{P}{B}\frac{\delta}{a+\Delta a}$		$G_{1C}(P,\delta,EI) = \frac{P^2}{BEI}\sqrt[3]{\left(\frac{3EI\,\delta}{2P}\right)^2}$	
Specimen	No Correc.	*xF/N*	No Correc.	$xF/N^{2/3}$
8 + 8_P1	309 ± 3.5	302.6 ± 3.1	336.7 ± 4.1	321.6 ± 3.8
8 + 8_P2	310.3 ± 8.8	303.4 ± 8.8	310.2 ± 7.3	295.2 ± 6.8
8 + 8_P3	307.7 ± 4.5	301.2 ± 4.9	332 ± 6.6	316.9 ± 6.5
Average	309 ± 2.8	302.4 ± 2.7	326.3 ± 6.5	311.2 ± 6.4
4 + 4_P1	297.4 ± 14.5	273.2 ± 11.7	337.7 ± 17.4	286.2 ± 11.3
4 + 4_P2	307.9 ± 6.7	284.2 ± 6.5	340.6 ± 5.8	291.3 ± 6.2
4 + 4_P3	313.2 ± 12	287.8 ± 9.1	347 ± 14.3	294.3 ± 9.4
Average	306.5 ± 6.2	282 ± 5.2	342.1 ± 6.5	290.8 ± 4.5
2 + 2_P1	286.8 ± 31.8	196.5 ± 8.7	406.5 ± 61.2	217.3 ± 10.3
2 + 2_P2	302.7 ± 17	202.7 ± 4.1	403.7 ± 37.2	209.4 ± 7.4
2 + 2_P3	314.2 ± 19.8	213.4 ± 6.2	428.9 ± 42.4	226.6 ± 9.3
Average	301.2 ± 12	204.2 ± 4.6	413 ± 22.2	217.8 ± 5.4

the propagation phases, smooth.

3.1. Symmetric configurations

6 points have been taken for the evaluation of G_{1C} for the symmetric cases (8 + 8, 4 + 4 y 2 + 2), from the *P-δ* curves, at the propagation zone, between two values for a_m, a_1 = 57.5 mm and a_2=107.5 mm (Δa = 50

Table 3
Calculation of G_{1C} (J/m^2) using the General Formulation for Symmetric case (GFS), without and with the effect of blocks.

	$G_{1C} = f(\delta, P, EI)$					
	8 + 8		4 + 4		2 + 2	
	No Blocks	Blocks	No Blocks	Blocks	No Blocks	Blocks
P1	335.4 ± 4.1	329.6 ± 3.8	329.4 ± 13.3	311.8 ± 12.2	347.6 ± 27.1	306.8 ± 26.3
P2	309 ± 7.3	303.8 ± 7.3	332.8 ± 7.8	314.9 ± 7.4	345.9 ± 8.6	305.3 ± 10.5
P3	330.7 ± 6.7	325.1 ± 7	339.3 ± 11	320.6 ± 9.9	366.2 ± 13.9	322.5 ± 14.4
Average	325.1 ± 6.5	319.5 ± 6.4	334.1 ± 5.4	316 ± 4.9	353.2 ± 9.4	311.5 ± 9.1

Table 4
Correction of *a* (mm) from experimental measurements using ASTM and GFS.

	Correction for *a* (Δa)					
	8 + 8		4 + 4		2 + 2	
	ASTM	GFS	ASTM	GFS	ASTM	GFS
P1	8.9	4.1 ± 0.9	7.3	4.8 ± 0.8	7.9	3.4 ± 0.6
P2	5.9	8.6 ± 0.9	3.4	3.2 ± 0.8	3.7	4.4 ± 1
P3	8.9	5 ± 1	4.1	4 ± 1.1	4.0	3.2 ± 0.7
Average	7.9	5.9 ± 1.1	4.9	4.1 ± 0.5	5.2	3.7 ± 0.4

mm). The values of P and δ associated with the measured crack length a (a_m) are those shown in Table 1.

The results of G_{1C} for the symmetric cases are shown in Table 2. They have been obtained applying the traditional procedures, without considering correction for large displacements or the effect of the gripping system and considering them. Tolerance has been calculated based on a 95% confidence level.

In view of the results, it is observed that for the specimens with greater bending stiffness (8 layers) the results are similar to those of all the procedures, not happening in this way as the number of layers is reduced.

Table 3 shows the results obtained when applying the GFS to the calculation of G_{1C}. The results shown and nominated as No Blocks correspond with those obtained with the calculations performed as in absence of blocks ($c = t = 0$ in connection to Fig. 6).

The average values indicated in the previous tables as well as the confidence level have been calculated using all the points of the series of 3 coupons (total 18 points). The small dispersion found supports the results obtained. It is also found that the nonconsideration of the loading blocks has a more pronounced effect as the specimen becomes more flexible.

As was already commented previously, the procedure with the GFS taking into account the effect of the blocks only needs to be fed with P, δ, E_f and the thickness of the layers to obtain not only the value of G_{1c} but also the value of a. This value would actually correspond to the crack length, considering that the end is clamped (a_c). For each of the values of a registered in the experimental study (a_m ranging from 57.5 to 107.5) the values of P and δ were recorded (Table 1) and for each pair a value of a was obtained (a_c). In Table 4, the mean of the values obtained for the 6 points considered per specimen is shown for each specimen.

As can be seen, the correction of the crack length is similar to the procedure used by ASTM and that of the GFS.

In order to verify that the beam model, together with its hypotheses, leads to results accurate enough, a FEM model has been developed. The idea is to feed the FEM model with a certain crack length and the load associated with it (P_{exp}) and to obtain the displacement δ.

The FEM model has been developed using Abaqus. The loading blocks have been included in the model. The numerical model has been analyzed as a plain stress problem. 91,262 nodes and 87,240 CPS4I elements have been used in the model. The mesh for the 1.53 mm laminate and the boundary conditions are shown in Fig. 9(a). The associated deformed shape for a 47.82 N load is shown in Fig. 9(b).

Two crack lengths have been used to feed the FEM model, the measured crack length $a_m = 57.5$ and the calculated crack length using GFS, a_c, for each configuration (see Table 5). In this way, two values have been obtained for δ with the FEM model for each configuration (δ_{FEM} for a_c and δ_{FEM} for a_m). It can be observed that the δ_{FEM} obtained using a_c is closer to δ_{exp} than δ_{FEM} obtained using a_m.

The presented procedure avoids having to measure the crack length, but it can be argued that this is not cost free, as requires introducing another measurement into the procedure, which is E_f. The measurement

Table 5
Separation of the adherents at the gripping zone (δ, *mm*) as a function of the crack length (mm) and P (N).

	Average Values		
	8 + 8	4 + 4	2 + 2
P_{exp}	47.8	18.5	7.9
a_m	57.5	57.5	57.5
a_c	63.9	61.8	61.8
δ_{FEM} for a_m	6.1	15.2	31.9
δ_{FEM} for a_c	8.2	18.4	37.7
δ_{exp}	7.2	17.1	36.5

of E_f may imply a variation associated with the nature of the material or simply errors in the measurement. Although this variation is not very large (the standards typically admits variations of an order of 10%), it seems pertinent to carry out a study of the incidence that this variation may have on the G_{1C} value. In this way, a parametric study has been carried out to evaluate the influence that deviations until 15% in E_f have on the interlaminar fracture toughness value obtained for the symmetric configurations. In the graph of Fig. 10, these errors are shown and, as can be seen, they are less than 5% in extreme cases (15%) and less than 2% in the common situations of having deviations/errors in E_f of 5%.

3.2. Nonsymmetric configurations.

As in the previous cases, 6 points have been taken in the propagation zone, between two values for a_m, taking a_1 equal to 57.5 mm and a_2 equal to 107.5 mm ($\Delta a = 50$ mm). The corresponding values of P (N) and δ (mm) are shown in Table 6.

In this case, the classical procedures are not applicable. The G_C values obtained using the GFNS are shown in Table 7.

These values, as expected, are higher than those obtained for the symmetric case, as $G_C \geq G_{1C}$. To obtain G_{1C}, the use of phenomenological laws seems to be a good option. Specifically, Hutchison and Suo [4] proposed several phenomenological expressions. The most used ones are going to be considered in this work:

$$\frac{G_C}{G_{1C}} = 1 + \tan^2(1-\lambda)\,\psi \tag{44}$$

$$\frac{G_C}{G_{1C}} = \frac{1}{1 + (\lambda - 1)sen^2\psi} \tag{45}$$

where λ is a parameter that collects the contribution of mode II on the criterium and ψ is the mixity of the modes.

There are several proposals to measure this mixity, the most common being to use a measurement from the stress field through the Stress Intensity Factor (SIF), ψ_K (46) (which is the way in which it intervenes in the laws of the equations (44) and (45), $\psi = \psi_K$). An alternative is to measure it from the energy release rate, ψ_G (47):

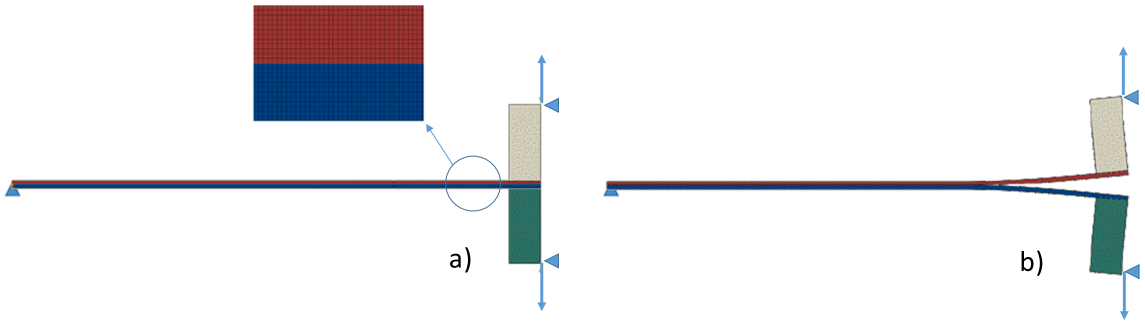

Fig. 9. (a) FEM mesh for $h_1 = 1.53$ mm laminate, (b) Deformed shape for $h_1 = 1.53$ mm, $a = 57.5$ mm and $P = 47.82$ N case.

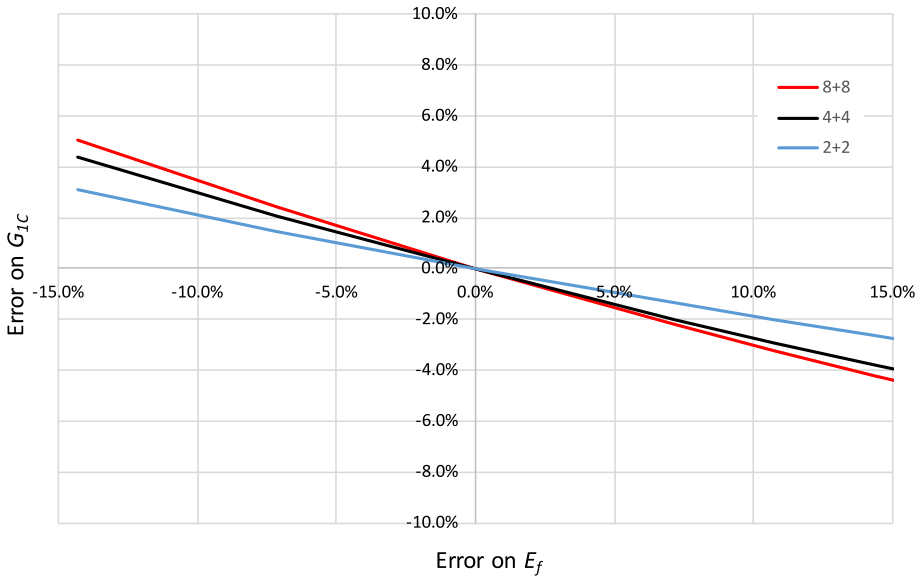

Fig. 10. Parametric study of the error committed in estimating G_C with the evolution of the error committed in E_f.

Table 6
Experimental measurements for nonsymmetric coupons.

	4 + 8 Layers					
	4 + 8_1		4 + 8_2		4 + 8_3	
a_m	P	δ	P	δ	P	δ
57.5	27.7	15.7	25.4	16.1	27.1	16.7
67.5	24.4	21.8	22.7	23.1	23.4	23.8
77.5	22.0	28.8	20.9	29.8	21.2	30.2
87.5	19.5	36.6	19.1	37.4	19.0	38.3
97.5	17.6	45.5	17.0	46.2	17.8	45.3
107.5	16.2	54.6	16.2	56.9	16.2	57.6

Table 7
G_C (J/m^2) calculated using GFNS for nonsymmetric configuration.

	$G_C = f(\delta, P, EI)$	
	4 + 8	
	No Blocks	Blocks
P1	471.3 ± 17.7	449.4 ± 16.1
P2	457.1 ± 34.5	436 ± 31.9
P3	473.2 ± 25.5	454.1 ± 16.9
Average	467.2 ± 12.5	446.5 ± 10.9

$$\tan\psi_K = \left|\frac{\tau(x,0)}{\sigma(x,0)}\right|_{x->0} = \left|\frac{K_{II}}{K_I}\right| \tag{46}$$

$$\tan^2\psi_G = \frac{G_{II}}{G_I} \tag{47}$$

where $\times$ is the distance measured from the crack tip, σ are and τ the normal and tangential components of the stress vector at a point of the interface, K_I and K_{II} are the stress intensity factors associated with I and II fracture modes, and G_I and G_{II} are the energy release rates associated with I and II fracture modes.

For the case of orthotropic materials and $\times$ and y being the orthotropy axes, the relation between ψ_K and ψ_G is given by [24]:

$$\tan\psi_K = \sqrt[4]{\frac{E_{11}}{E_{22}}}\tan\psi_G \tag{48}$$

The mixity ψ_G is independent on the material and can be approximated by expression (49) [5].

$$\psi_G(^\circ) = 33.927^\circ\left(\frac{h_1}{h_2}\right)^3 - 66.586^\circ\left(\frac{h_1}{h_2}\right)^2 - 5.276^\circ\left(\frac{h_1}{h_2}\right) + 37.996^\circ \tag{49}$$

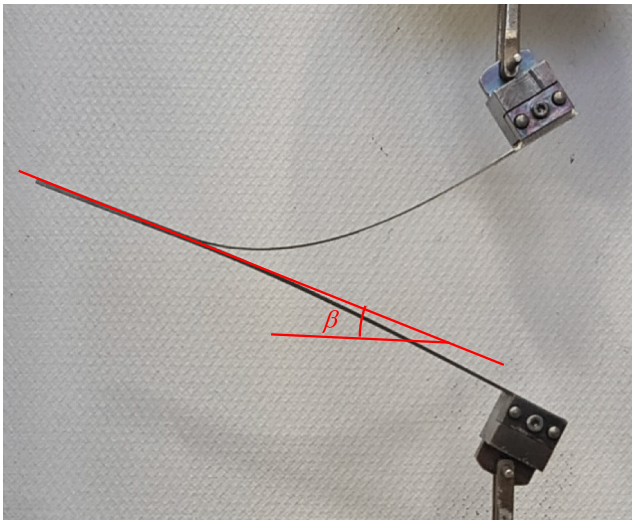

Fig. 11. Experimental measurement of angle β.

Table 8
Values of G_C (J/m^2) and G_{1C} (J/m^2) calculated for nonsymmetric coupons.

			$E_{11} = 165$ GPa $E_{22} = 9.3$ GPa	λ for $G_{2C}/G_{1C} = 2.6$		G_C/G_{1C}			G_{1C_avg}			Error (%)	
Conf	h_1/h_2	ψ_G (°)	ψ_K (°)	Proc. 1	Proc. 2	Proc. 1	Proc. 2	G_{C_avg}	Proc. 1	Proc. 2	$G_{1C\_sym\_avg}$	Proc. 1	Proc. 2
4 + 8	0.5	22.95	41	0.416	0.369	1.20	1.37	446.5	372.9	325.3	315.6	18%	3%

Table 9
Comparison of the β angles (º) experimentally measured and calculated as a function of a_m (mm).

	a_m			
	87.5	97.5	107.5	117.5
β_{avg} calculated for 4 + 8_P1	12.4	13.7	14.9	16.7
β_{avg} calculated for 4 + 8_P2	12.6	13.7	15.3	16.9
β_{avg} calculated for 4 + 8_P3	12.7	13.8	15.4	16.8
β_{avg} calculated	12.6	13.7	15.2	16.8
β_{exp} for 4 + 8_P2	11.8	13.4	14.8	16.2

For the case under conideration, h_1/h_2 is equal to 0.5, obtaining, in this way, a mixity of 23° for ψ_G. Using now E_{11} (165 GPa) and E_{22} (9.5 GPa) in (48), a value of $\psi_K = 41°$ is obtained.

To get a plausible value of λ, the minimum nominal values of G_{1C} and G_{2C} of this material can be used. Thus, in this case, the minimum values of G_{1C} and G_{2C} that the material have to meet are 240 and 650 J/m^2, respectively, according to material standards used by aeronautical manufacturing companies. Particularizing Eqs. (44) and (45) for $\psi_K = 90°$ ($G_C = G_{2C}$) and assuming for G_{1C} and G_{2C} the minimum values stablished by the standard, a value of λ is obtained, for each expression. In what follows, we will call Procedure 1 to that associated with the use of equation (44) and Procedure 2 to that associated with the use of equation (45).

Table 8 shows the values of λ and G_{1C} obtained using Procedure 1 and Procedure 2. Accepting that G_{1C} is a property of the material and thus that obtained in the symmetric case can be used as a reference ($G_{1C\_avg} =$ 315.7 J/mˆ2, Table 3), an error in the estimation of G_{1C} using procedures 1 and 2 can be calculated, according to equation (50).

$$Error\ (\%) = 100\frac{G_{1C\_avg} - G_{1C\_sym\_avg}}{G_{1C\_sym\_avg}} \tag{50}$$

It can be seen, Table 8, that G_{1C} calculated using Procedure 2 estimates best the value expected, that is, the one obtained for the symmetric configurations.

On the way of supporting the GFNS, as it has been based in many hypotheses, it could be desirable to compare a magnitude associated to the test that can be easily measured different to that used in the calculations (P and δ). The angle that the axis of the specimen adopts during the loading process seems to be a good candidate. This angle has been experimentally measured (angle β shown in Fig. 11).

The values of β that appear in the first 3 rows of Table 9 have been obtained applying GFNS for each of the specimens, from the values of P and δ associated with the a indicated in the upper part of the table (a_m). With these values, the average value of β (β_{avg}) indicated in the 4th row of the table is obtained. The last row shows the experimentally measured value of β for specimen 2, for comparison purposes, at the same positions. A satisfactory agreement between both values can be observed.

4. Conclusions

A general formulation, able to be applied to symmetric (GFS) and nonsymmetric (GFNS) composite laminates, to determine the interlaminar fracture toughness has been proposed. These formulations allow a fast and precise evaluation of G_C in DCB tests to be performed, avoiding the measurement of a, which facilitates the performance and the data acquisition of the tests.

It has to be remarked that, for the case of nonsymmetric configurations, the formulation developed represents a new approach to calculate the interlaminar fracture toughness, involving in the formulation the presence of loading blocks.

An experimental campaign of DCB tests for symmetric and nonsymmetric configurations involving different thicknesses of the adherents has been carried out.

For symmetric configurations, the values obtained using the procedure developed without the necessity of measuring the crack length a (GFS), have been compared with those obtained from classical existing formulations. For the range of thicknesses considered in the standards, the values obtained from previous and presented formulations are similar, which validates the GFS procedure proposed in this paper. For small thicknesses the values of the interlaminar fracture toughness obtained with the previous procedures (even considering the use of correction factors) are different to that obtained for standard thicknesses, whereas the values obtained with the procedure proposed in this work coincide, which is coherent with the idea that G_{1C} is a property of the material, independently on the adherent thicknesses.

For nonsymmetric configurations, the new procedure developed (GFNS) allows G_C to be obtained. The determination of G_{1C} from G_C requires the use of a phenomenological law involving the mixity of the fracture mode. Two phenomenological laws from Hutchison and Suo have been used, leading to different results. One of them is very close to that obtained for symmetric configurations, which is very consistent with the idea that G_{1C} is a material property.

CRediT authorship contribution statement

J. Cañas: Conceptualization, Methodology, Investigation, Validation, Writing – review & editing. **J. Justo:** Conceptualization, Methodology, Investigation, Writing – review & editing, Funding acquisition. **F. París:** Writing – review & editing, Supervision, Funding acquisition.

Declaration of Competing Interest

The authors declare that they have no known competing financial interests or personal relationships that could have appeared to influence the work reported in this paper.

Acknowledgements

This work was supported by the Junta de Andalucía (Consejería de Economía y Conocimiento) (Projects P18-FR-3855 and P18-FR-3360).

References

[1] ASTM-D5228-13. Standard test method for mode I interlaminar fracture toughness of unidirectional fiber-reinforced polymer matrix composite; 2013.
[2] ISO 15024. Fibre-reinforced plastic composites-determination of mode I interlaminar fracture toughness, GIc, for unidirectionally reinforced materials; 2001.
[3] Airbus, AITM 1-0005. Carbon fiber reinforced plastics. Determination of interlaminar fracture toughness energy. Mode I. (G_{IC} Test); 2015.
[4] Hutchinson JW, Suo Z. Mixed mode cracking in layered materials. Adv Appl Mech 1992;29:63–191.
[5] Cañas J, Blázquez A, Estefani A, Távara L. Accurate determination of the stiffness properties for an elastic interface under peeling conditions between, homogeneous materials. Compos Struct 2022;285:115106. https://doi.org/10.1016/j.compstruct.2021.115106.
[6] Williams JG. Large displacement and end block effects in the DCB interlaminar test in modes I and II. J Compos Mater 1987;21:330–47.
[7] Williams JG. On the calculation of energy release rates for cracked laminates. Int J Fract 1988;36:101–19.
[8] Williams JG. The fracture mechanics of delamination test. J Strain Anal 1989;24(4):207–14.
[9] Paris AJ, Gunderson JD. DCB test for the interlaminar fracture toughness of composites. In: Proceedings of the eighteenth international conference on composites engineering (ICCE-18), Anchorage, Alaska, July 4–10; 2010.
[10] Franklin VA, Christopher T. Fracture energy estimation of DCB specimens made of glass/epoxy: an experimental study. Adv Mater Sci Eng 2013. https://doi.org/10.1155/2013/412601.
[11] Tamuzs V, Tarasovs S, Vilks U. Delamination properties of translaminar-reinforced composites. Compos Sci Technol 2003;63:1423–31.
[12] Biel A, Sitgh U. An analysis of the evaluation of the fracture energy using the DCB-specimen. Arch Mech 2007;59(4–5):311–27.
[13] Xu W, Guo ZZ, Yu Y, Xiong J, Gao Y. Experimental and analytical characterizations of finite interlaminar crack growth of 2D woven textile composites. Compos Struct 2018;206:713–21.
[14] Xu W, Guo ZZ. A simple method for determining the mode I interlaminar fracture toughness of composites without measuring the growing crack length. Eng Fract Mech 2018;191:476–85.

[15] Kanninen MF. An augmented double cantilever beam model for stud crack propagation and arrest. Int J Fract 1973;9(1):83–92.
[16] Kanninen MF. A dynamic analysis of unstable crack propagation and arrest in the DCB test specimen. Int J Fract 1974;10(3):415–30.
[17] Pavelko V, Lapsa K, Pavlovskis P. Determination of the mode I interlaminar fracture toughness by using a nonlinear double-cantilever beam specimen. Mech Compos Mater 2016;52(3):347–58.
[18] Ding JC, Xu W. Determination of mode I interlaminar fracture toughness of composite by a wedge-insert double cantilever beam and the nonlinear J integral. Compos Sci Technol 2021;206:108674.
[19] Xu W, Ding JC. Correction of the large displacement effect on determination of mode I interlaminar fracture toughness of composite. Eng Fract Mech 2020;238:107279.
[20] Sundararaman V, Davidson BD. An unsymmetric double cantilever beam test for interfacial fracture toughness determination. Int J Solids Struct 1997;34(7):799–817.
[21] ISO 14125:1998. Fibre-reinforced plastics composites. Determination of flexural properties; 1998.
[22] EN 2561:1995. Aerospace series. Carbon fibre reinforced plastics. Unidirectional laminates. Tensile test parallel to the fibre direction; 1995.
[23] EN 2597:1998. Aerospace series. Carbon fibre reinforced plastics. Unidirectional laminates. Tensile test perpendicular to the fibre direction; 1998.
[24] Mantic V, París F. Relation between SIF and ERR based measures of fracture mode mixity in interface cracks. Int J Fract 2004;130:557–69.